

Ruthenium Complexes Containing Bis(diarylamido)/Thioether Ligands: Synthesis and Their Catalysis for the Hydrogenation of Benzonitrile

Shin Takemoto,[§] Harumi Kawamura,[†] Yoshiaki Yamada,[†] Takayoshi Okada,[†] Atsushi Ono,[†] Eri Yoshikawa,[†] Yasushi Mizobe,[‡] and Masanobu Hidai^{*,†}

Department of Materials Science and Technology, Faculty of Industrial Science and Technology, Science University of Tokyo, Noda, Chiba 278-8510, Japan, and Institute of Industrial Science, The University of Tokyo, Komaba, Meguro-ku, Tokyo 153-8505, Japan

Received April 29, 2002

Treatment of the thioethers (RNH-*o*-C₆H₄)₂S (H₂[R₂NSN]; R = Xy, Xyf; Xy = 3,5-Me₂C₆H₃, Xyf = 3,5-(CF₃)₂C₆H₃) with 2 equiv of *n*-BuLi followed by addition of 0.5 equiv of [(η^6 -C₆H₆)-RuCl₂]₂ in THF gave the bis(diarylamido)/thioether complexes [(η^6 -C₆H₆)Ru[R₂NSN]] (R = Xy (**1a**), R = Xyf (**1b**)) in moderate yields. In the presence of **1a** (1 mol %) and PCy₃ (2 mol %; Cy = cyclohexyl), benzonitrile was catalytically hydrogenated to give benzylamine (72%) and benzylidenebenzylamine (27%) at 80 °C and 30 atm, while the hydrogenation with **1b** as a catalyst precursor resulted in the formation of benzylamine (37%) and benzylidenebenzylamine (51%) under the same reaction conditions. The yield of benzylamine was improved up to 92% by using a catalyst mixture of **1a** (1 mol %)/PCy₃ (2 mol %)/*t*-BuONa (10 mol %). On the other hand, the reaction of **1a** with excess PMe₃ afforded the tris(trimethylphosphine) derivative [(PMe₃)₃Ru[Xy₂NSN]] (**2**). Treatment of **2** with excess PhCN, MeCN, or N₂H₄·H₂O resulted in the replacement of a PMe₃ ligand by these substrates to give [(PMe₃)₂LRu[Xy₂NSN]] (**3**, L = PhCN; **4**, L = MeCN; **5**, L = N₂H₄), while the reaction of **2** with benzoylhydrazine gave the κ^2 -benzoylhydrazido complex [(PMe₃)₂Ru(κ^2 -(*O,N*)-PhC(O)=NNH₂)(H[Xy₂NSN])] (**6**). Structures of **1a**, **1b**, **2**, **5**, and **6** have been determined by X-ray crystallography.

Introduction

Amido–metal bonds in late transition metal amido complexes are known to react with dihydrogen to form amine–hydride species.¹ This process corresponds to the heterolytic cleavage of dihydrogen by the aid of an amido–metal bond to create a protonic N–H hydrogen and a hydride on the metal. For instance, Fryzuk and co-workers demonstrated that the ruthenium(II) complex [RuCl(PPh₃)₂(Ph₂PCH₂SiMe₂)₂N]} containing a tridentate amido/bis(phosphine) ligand produces an amine–hydride complex [RuHCl(PPh₃)₂(Ph₂PCH₂SiMe₂)₂NH]} upon treatment with dihydrogen.² More recently, Morris et al. have characterized the ruthenium(II) amido–hydrido complex [RuH(NHCMe₂CMe₂NH₂)(*R*-binap)] (binap = 2,2′-bis(diphenylphosphino)-1,1′-binaphthyl), which gives the diamine–dihydrido complex [RuH₂(NH₂-CMe₂CMe₂NH₂)(*R*-binap)] under H₂.³ The latter reaction provides evidence for involvement of the heterolytic cleavage of dihydrogen on a Ru–N bond in the hydrogenation of ketones, aldehydes, and imines catalyzed

by the ruthenium(II) complex/diamine/KOH mixture recently developed by Noyori et al.⁴ These findings show the importance of heterolytic H₂ activation for the hydrogenation of C=O and C=N polar bonds. Thus, we presume that late transition metal amido complexes serve as catalysts for hydrogenation of a variety of polar unsaturated substrates other than ketones and imines. We have long been interested in hydrogenation of the N≡N triple bond of dinitrogen, which is polarized when coordinated to a metal center in an end-on fashion.⁵ Previously, we have reported the reaction of the tungsten dinitrogen complex *cis*-[W(N₂)₂(PMe₂Ph)₄] with acidic ruthenium η^2 -dihydrogen complexes, which leads to the protonation of the coordinated dinitrogen on tungsten by the heterolytic cleavage of the coordinated dihydrogen on ruthenium.^{6,7} The reaction results in the formation of ammonia from N₂ and H₂; however, electrons for the reduction of N₂ are supplied from tungsten and the reaction is thus stoichiometric. We have now turned our attention to amido complexes of late transition metals aiming at development of metal complexes that effectively coordinate and activate both N₂ and H₂ molecules. In this paper, we report the synthesis of

[†] Science University of Tokyo.

[‡] The University of Tokyo.

[§] Present address: Department of Materials Science, Faculty of Integrated Arts and Sciences, Osaka Prefecture University, Sakai, Osaka 599-8531, Japan.

(1) Fryzuk, M. D.; Montgomery, C. G. *Coord. Chem. Rev.* **1989**, *95*, 1–40.

(2) Fryzuk, M. D.; Montgomery, C. G.; Rettig, S. J. *Organometallics* **1991**, *10*, 467–473.

(3) Abdur-Rashid, K.; Faatz, M.; Lough, A. J.; Morris, R. H. *J. Am. Chem. Soc.* **2001**, *123*, 7473–7474.

(4) Noyori, R.; Ohkuma, T. *Angew. Chem., Int. Ed.* **2001**, *40*, 40–73.

(5) (a) Hidai, M.; Mizobe, Y. *Chem. Rev.* **1995**, *95*, 1115–1133. (b) Hidai, M. *Coord. Chem. Rev.* **1999**, *186*, 99–108.

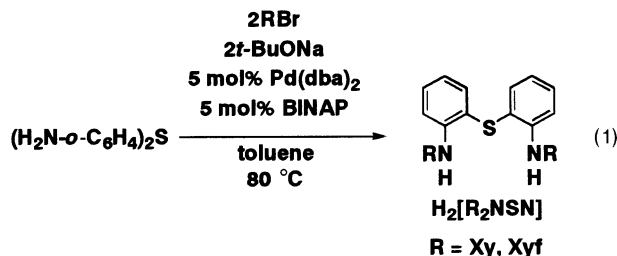
(6) (a) Nishibayashi, Y.; Iwai, S.; Hidai, M. *Science* **1997**, *297*, 540–542. (b) Nishibayashi, Y.; Takemoto, S.; Iwai, S.; Hidai, M. *Inorg. Chem.* **2000**, *39*, 5946–5957.

(7) Hidai, M.; Mizobe, Y. *Pure Appl. Chem.* **2001**, *73*, 261–263.

ruthenium complexes containing tridentate bis(diaryl-amido)/thioether ligands $[(\text{RN}-o\text{-C}_6\text{H}_4)_2\text{S}]^{2-}$ ($[\text{R}_2\text{NSN}]^{2-}$; $\text{R} = \text{Xy}$, Xyf ; $\text{Xy} = 3,5\text{-Me}_2\text{C}_6\text{H}_3$, $\text{Xyf} = 3,5\text{-(CF}_3)_2\text{C}_6\text{H}_3$) and their catalysis for hydrogenation of the $\text{C}\equiv\text{N}$ triple bond of benzonitrile, whose structure has some relevance to that of the metal-bound dinitrogen molecule.

Results and Discussion

Synthesis of $\text{H}_2[\text{R}_2\text{NSN}]$ and $[(\eta^6\text{-C}_6\text{H}_6)\text{Ru}[\text{R}_2\text{NSN}]]$ ($\text{R} = \text{Xy}$, Xyf). The ligand precursor ($\text{XyNH}-o\text{-C}_6\text{H}_4)_2\text{S}$ ($\text{H}_2[\text{Xy}_2\text{NSN}]$) was prepared by the palladium-catalyzed coupling reaction⁸ between the diamine ($\text{H}_2\text{N}-o\text{-C}_6\text{H}_4)_2\text{S}$ and 2 equiv of 5-bromo-*m*-xylene (eq 1). The



product was isolated as a yellow oil in ~75% yield after purification by flash chromatography on silica gel. An analogous thioether $\text{H}_2[\text{Xyf}_2\text{NSN}]$ containing 3,5-(CF_3)₂ C_6H_3 groups (Xyf) was also synthesized in a similar manner. The ligands of this type were originally developed by Schrock et al., who recently reported the synthesis of a series of group 4 metal complexes containing $[(\text{RN}-o\text{-C}_6\text{H}_4)_2\text{S}]^{2-}$ ($\text{R} = i\text{-Pr}$, $t\text{-Bu}-d_6$)⁹ ligands as well as the ether analogues $[(\text{RN}-o\text{-C}_6\text{H}_4)_2\text{O}]^{2-}$ ($\text{R} = i\text{-Pr}$, Cy , $t\text{-Bu}-d_6$, 2,4,6- $\text{Me}_3\text{C}_6\text{H}_2$)^{10,11} and demonstrated that the zirconium complex $[(t\text{-Bu}-d_6\text{-N}-o\text{-C}_6\text{H}_4)_2\text{O}]\text{-ZrMe}(\text{PhNMe}_2)[\text{B}(\text{C}_6\text{F}_5)_4]$ initiates the living polymerization of 1-hexene.¹² We have chosen the bis(diaryl-amido)/thioether ligand system for an entry into amidoruthenium chemistry because the diarylamido ligands do not suffer from decomposition via the $\beta\text{-H}$ -elimination to imine-hydrides. Actually, we could not obtain any amidoruthenium complex from the reaction of $[(\eta^6\text{-C}_6\text{H}_6)\text{RuCl}_2]_2$ with 2 equiv of the in situ generated dilithium salt $\text{Li}_2[t\text{-Pr}_2\text{NSN}]$ in THF. However, when $\text{Li}_2[\text{Xy}_2\text{NSN}]$ was employed, the reaction proceeded smoothly to give the red crystalline bis(diaryl-amido)/thioether complex $[(\eta^6\text{-C}_6\text{H}_6)\text{Ru}[\text{Xy}_2\text{NSN}]]$ (**1a**) in ~60% yield after recrystallization from dichloromethane-methanol (eq 2). The ¹H NMR spectrum of **1a** exhibits a resonance for the C_6H_6 moiety at 4.41 ppm, which is characteristic of the η^6 -coordinated benzene ligand. The simple spectral pattern of the XyNC_6H_4 moieties including a singlet resonance for the methyl protons at 2.23 ppm indicates the presence of a plane of symmetry in the molecule. The tridentate coordination of the $[\text{Xy}_2\text{-}$

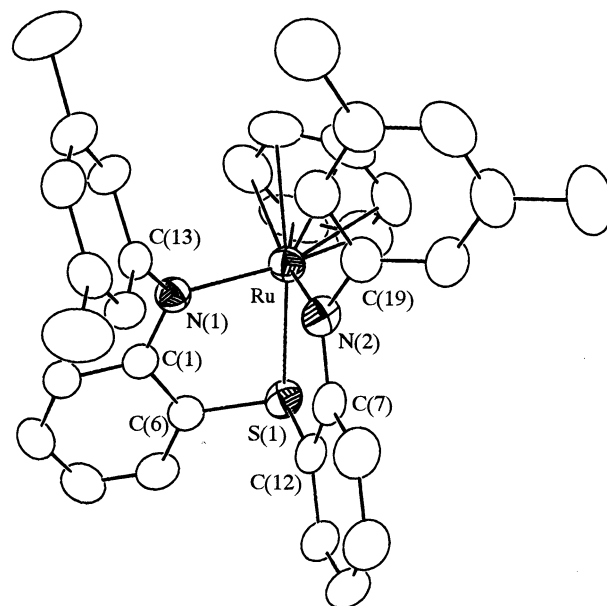
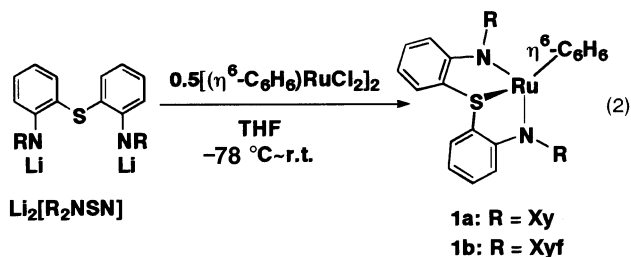


Figure 1. ORTEP diagram of **1a** drawn at the 50% probability level. Hydrogen atoms are omitted for clarity.

Table 1. Selected Bond Lengths (Å) and Angles (deg) for **1a** and **1b**

	1a	1b
Ru–N(1)	2.116(3)	2.123(3)
Ru–N(2)	2.070(3)	2.091(3)
Ru–S(1)	2.3277(11)	2.3310(7)
N(1)–C(1)	1.357(4)	1.379(4)
N(1)–C(13)	1.420(4)	1.409(4)
N(2)–C(7)	1.360(4)	1.371(4)
N(2)–C(19)	1.429(4)	1.408(4)
S(1)–C(6)	1.777(4)	1.777(3)
S(1)–C(12)	1.786(4)	1.783(3)
N(1)–Ru–N(2)	85.84(12)	86.05(10)
C(1)–N(1)–Ru	119.2(2)	118.69(19)
C(13)–N(1)–Ru	121.2(2)	120.54(19)
C(1)–N(1)–C(13)	117.4(3)	117.1(2)
C(7)–N(2)–Ru	119.9(2)	118.76(19)
C(19)–N(2)–Ru	117.6(2)	118.6(2)
C(7)–N(2)–C(19)	119.6(3)	118.8(3)
C(6)–S(1)–C(12)	103.72(16)	102.17(14)



$\text{NSN}]^{2-}$ ligand in **1a** was unequivocally confirmed by an X-ray analysis; the molecular structure of **1a** is shown in Figure 1, and the selected bond lengths and angles are listed in Table 1. The Ru–N distances of 2.070(3) and 2.116(3) Å are comparable to that of the Ru–sulfonamido bond observed for the 18-electron complex $[(p\text{-cymene})\text{RuX}(\text{TsNCHPhCHPhNH}_2)]$ ($\text{X} = \text{H}$, Cl),¹³ but longer than that of the Ru–alkylamido bond (1.897(6) Å) in the 16-electron complex $[(p\text{-cymene})\text{Ru}(\text{TsNCHPhCHPhNH})]$, in which a significant double-bond character of the Ru–N bond is implied.¹³ The sum

(8) (a) Wolfe, J. P.; Wagaw, S.; Buchwald, S. L. *J. Am. Chem. Soc.* **1996**, *118*, 7215–7216. (b) Louie, J.; Driver, M. S.; Hamann, B. C.; Hartwig, J. F. *J. Org. Chem.* **1997**, *62*, 1268–1273.

(9) Graf, D. D.; Schrock, R. R.; Davis, W. M.; Stumpf, R. *Organometallics* **1999**, *18*, 843–852.

(10) Baumann, R.; Stumpf, R.; Davis, W. M.; Liang, L.-C.; Schrock, R. R. *J. Am. Chem. Soc.* **1999**, *121*, 7822–7836.

(11) Liang, L.-C.; Schrock, R. R.; Davis, W. M. *Organometallics* **2000**, *19*, 2526–2531.

(12) Baumann, R.; Davis, W. M.; Schrock, R. R. *J. Am. Chem. Soc.* **1997**, *119*, 3830–3831.

(13) Haack, K.-J.; Hashiguchi, S.; Fujii, A.; Ikariya, T.; Noyori, R. *Angew. Chem., Int. Ed. Engl.* **1997**, *36*, 285–288.

Table 2. Hydrogenation of Benzonitrile^a

entry	catalyst	H ₂ (atm)	conv (%)	yield (%) ^{b,c}		
				PhCH ₂ NH ₂	(PhCH ₂) ₂ NH	PhCH=NCH ₂ Ph
1	1a /2PCy ₃	30	100	72	<1	27
2	1a /2PMe ₃	30	100	61	16	23
3	1a	30	7	0	<1	6
4	1a /2PCy ₃	60	100	67	<1	33
5	1a /2PCy ₃ /10 <i>t</i> -BuONa	30	98	92	4	2
6	1a /2PCy ₃ /10EtONa	30	98	88	<1	10
7	1b	30	<1	0	<1	<1
8	1b /2PCy ₃	30	90	37	1	51
9	1b /2PCy ₃	60	100	67	7	26
10	1b /2PCy ₃ /10 <i>t</i> -BuONa	30	98	85	<1	13
11	[RuH ₂ (H ₂) ₂ (PCy ₃) ₂]	30	95	80	6	3
12	3	30	100	49	16	34

^a Conditions: complexes **1a**, **1b**, [RuH₂(H₂)₂(PCy₃)₂], or **3** (0.050 mmol), THF (5 mL), benzonitrile (5.00 mmol), temperature 80 °C, time 18 h. ^b Determined by GLC. ^c Based on benzonitrile.

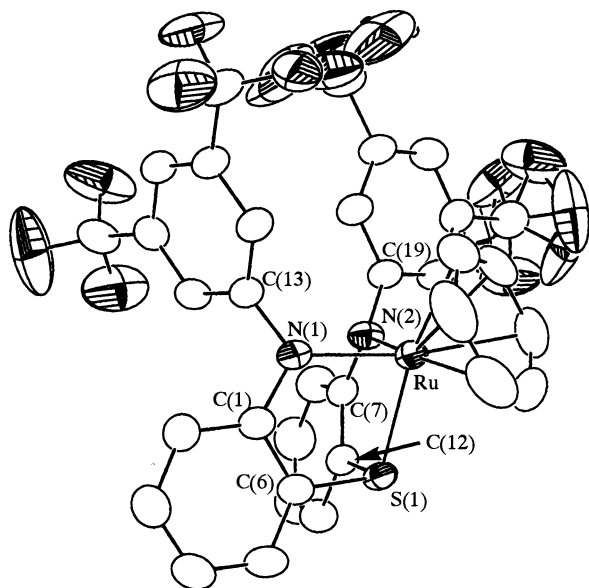


Figure 2. ORTEP diagram of **1b** drawn at the 50% probability level. Hydrogen atoms are omitted for clarity.

of bond angles around the N(1) and N(2) atoms are 357.8° and 357.1°, respectively, and these nitrogen atoms adopt almost planar geometry. The C–N bond lengths in the XyN moieties (1.420(4) and 1.429(4) Å) are longer than those in the NC₆H₄ units (1.357(4) and 1.360(4) Å). This indicates a larger degree of delocalization of the lone pair electrons on the amide nitrogen toward the phenylene ring than to the Xy ring.

A similar reaction between Li₂[Xyf₂NSN] and [(η^6 -C₆H₆)RuCl₂]₂ afforded an analogous complex [(η^6 -C₆H₆)Ru[Xyf₂NSN]] (**1b**) (eq 2) in ~40% yield. The structure of **1b** was also determined by an X-ray analysis (Figure 2 and Table 1). The bond lengths and angles around the ruthenium atom are almost the same as those observed for **1a**, and the geometries around the amide nitrogen atoms are also trigonal planar. The difference between the two C–N bond lengths in complex **1b** (~0.03 Å) is smaller than that of complex **1a** (~0.065 Å) (vide supra), probably due to the more electron-withdrawing nature of the Xyf ring than the Xy ring.

Hydrogenation of Benzonitrile Catalyzed by 1a or 1b. Although ruthenium complexes **1a** and **1b** adopt coordinatively saturated 18-electron configurations, the η^6 -C₆H₆ ligand is expected to be readily replaced by

other ligands, as established for many other arene–ruthenium(II) complexes.¹⁴ Thus, a solution of **1a** in THF was heated at 80 °C for 48 h in the presence of 2 equiv of PCy₃ (Cy = cyclohexyl) in an attempt to trap the nascent Ru[Xy₂NSN] species by PCy₃. After recrystallization from THF–hexanes a dark violet crystalline solid was obtained, which showed resonances ascribed to the PCy₃ and [Xy₂NSN]²⁻ ligands in 1:1 intensity ratio in its ¹H NMR spectrum and a singlet resonance at 62.0 ppm in the ³¹P{¹H} NMR spectrum. No signal assignable to the η^6 -C₆H₆ ligand was found in the ¹H NMR spectrum. These spectroscopic features suggest that the η^6 -C₆H₆ ligand in **1a** is displaced by 1 equiv of PCy₃ ligand during the reaction. However, the complexity in the ¹H NMR spectrum and failure to obtain suitable crystals for an X-ray analysis precluded further characterization of the product. Nevertheless, thermal displacement of the η^6 -C₆H₆ ligand with PCy₃ opens up potentially vacant coordination sites on ruthenium, which may be used for activation of dihydrogen and substrates. To test the potential of the Ru[Xy₂NSN] species as a hydrogenation catalyst, benzonitrile was hydrogenated by using **1a** as a catalyst precursor. The results are summarized in Table 2. In the presence of 1 mol % of **1a** and 2 mol % of PCy₃, benzonitrile was smoothly hydrogenated at 80 °C in THF under 30 atm of H₂ with 100% conversion within 18 h to give benzylamine in 72% yield together with benzylidenebenzylamine (27%) and a trace amount of dibenzylamine (entry 1). These minor products are considered to arise from the nucleophilic addition of benzylamine to the coordinated benzonitrile or benzaldehyde imine and subsequent ammonia elimination/hydrogenation processes.¹⁵ In place of PCy₃, trimethylphosphine can be used as a coligand. The catalyst **1a**/2PMe₃ exhibited almost the same activity as **1a**/2PCy₃, but caused formation of an increased amount of dibenzylamine (entry 2). In the absence of the phosphine ligand, complex **1a** showed a very low catalytic activity (entry 3). For the hydrogenation with the **1a**/2PCy₃ catalyst system, increase of the initial H₂ pressure from 30 to 60 atm did not largely affect the product selectivity (entry 4). However, the selectivity toward benzylamine was remarkably improved when *t*-BuONa or EtONa (10

(14) Doucet, H.; Ohkuma, T.; Murata, K.; Yokozawa, T.; Kozawa, M.; Katayama, E.; Englang, A. H.; Ikariya, T.; Noyori, R. *Angew. Chem., Int. Ed.* **1998**, *37*, 1703–1707.

(15) Bianchini, C.; Santo, V. D.; Meli, A.; Oberhauser, W.; Psaro, R.; Vizza, F. *Organometallics* **2000**, *19*, 2433–2444.

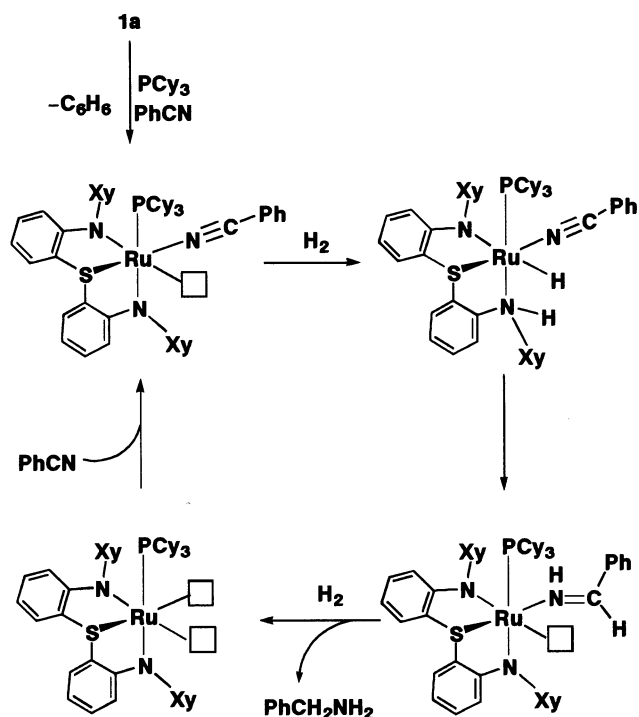
mol %) was added as a catalyst component (entries 5 and 6). We presume that the alkoxide base abstracts the NH proton from the ruthenium amine–hydride species derived from the heterolytic cleavage of dihydrogen by the amidoruthenium complex to generate the anionic hydridoruthenate species, which may promote the hydride transfer to the cyano carbon of benzonitrile much faster than the nucleophilic attack of benzylamine.

To explore the effect of the substituent of amide ligands on the catalytic performance, we employed **1b** as a catalyst precursor. Although complex **1b** itself was a very poor precatalyst (entry 7), the catalytic activity of **1b**/2PCy₃ was as high as that of **1a**/2PCy₃ (entry 8). In contrast to the **1a**/2PCy₃ catalyst system, the catalyst **1b**/2PCy₃ produced benzylidenebenzylamine as a major product. When the hydrogenation was conducted with the initial H₂ pressure of 60 atm, the product selectivity was shifted to benzylamine (entry 9). Therefore, we presume that the electronic nature of the substituents on the amide nitrogen affects both the reactivity of the amidoruthenium species toward dihydrogen and the relative rate of the hydride transfer and the nucleophilic attack of benzylamine to the coordinated benzonitrile. Similarly to the **1a**/2PCy₃/10*t*-BuONa catalyst system, the catalyst **1b**/2PCy₃/10*t*-BuONa also produced benzylamine in high selectivity (entry 10).

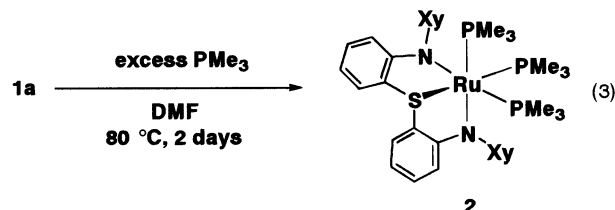
There are several reports on the homogeneous hydrogenation of benzonitrile catalyzed by ruthenium complexes. The complex [(triphos)Ru(NCMe)₃](CF₃SO₃)₂ (triphos = (Ph₂PCH₂)₃Me) has been reported to yield benzylidenebenzylamine in high selectivity,¹⁵ while the anionic hydridoruthenate complex K[(Ph₃P)₂(Ph₂PC₆H₄)-RuH₂] has been known to produce benzylamine as a sole product.¹⁶ To reveal the role of the amide–ruthenium bond in the hydrogenation of benzonitrile presented here, we employed [RuH₂(η²-H₂)₂(PCy₃)₂]¹⁷ as a reference catalyst, which showed a catalytic activity comparable to that of **1a**/2PCy₃, but the product distribution was different (entry 10). We conclude that the active catalyst species derived from **1a**/2PCy₃ is not the same as that formed from [RuH₂(η²-H₂)₂(PCy₃)₂], but probably contains amide–ruthenium bond(s) because the ¹H NMR spectrum of the reaction mixture of the hydrogenation of benzonitrile with **1a**/2PCy₃ did not exhibit resonances ascribed to the free thioether ligand H₂[Xy₂NSN]. The finding that the product distribution is significantly affected by the kind of substituent on the amide ligands also supports the catalysis by an amidoruthenium species. A plausible reaction mechanism for the hydrogenation of benzonitrile with the **1a**/2PCy₃ catalyst system is depicted in Scheme 1, which includes the heterolytic activation of dihydrogen on the Ru–N bond and the subsequent transfer of H⁺ and H⁻ to the coordinated nitrile.

Synthesis and Reactivities of [(PMe₃)₃Ru[Xy₂NSN]]. Although we could not characterize the product formed from the reaction between **1a** and PCy₃ (vide infra), treatment of **1a** with an excess amount of trimethylphosphine (10 equiv) in DMF at 80 °C for 2 days afforded the tris(trimethylphosphine) derivative

Scheme 1

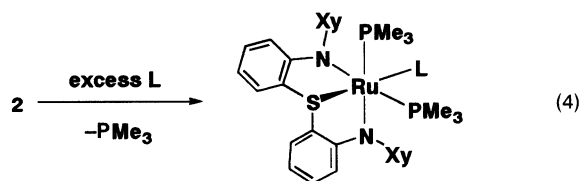


[(PMe₃)₃Ru[Xy₂NSN]] (**2**), which was isolated as yellow crystals in ~70% yield (eq 3). The ³¹P{¹H} NMR



spectrum of **2** revealed two phosphorus resonances at 2.2 and –12.9 ppm as a doublet and a triplet, respectively, indicating the presence of three phosphorus nuclei, of which two are chemically equivalent. The ¹H NMR spectrum of **2** showed a methyl resonance for the unique PMe₃ ligand at 0.53 ppm as a doublet, and that for the remaining two PMe₃ ligands was found at 1.11 ppm as a weakly coupled virtual triplet. An X-ray diffraction study shows that the structure of **2** is distorted octahedral and the [Xy₂NSN]²⁻ ligand adopts *fac* geometry (Figure 3, Table 3). The Ru–N bond lengths are ~0.1 Å as long as those in **1a**.

When complex **2** was treated with benzonitrile, the PMe₃ ligand located at the position trans to the sulfur atom was selectively substituted to give the benzonitrile complex [(PMe₃)₂(PhCN)Ru[Xy₂NSN]] (**3**) in 49% yield (eq 4). The ³¹P{¹H} NMR spectra of **3** displayed a singlet



- 3**: L = PhCN
4: L = MeCN
5: L = N₂H₄

(16) Grey, R. A.; Pez, G. P.; Wallo, A. *J. Am. Chem. Soc.* **1981**, *103*, 7536–7542.

(17) Chaudret, B.; Poilblanc, P. *Organometallics* **1985**, *4*, 1722–1726.

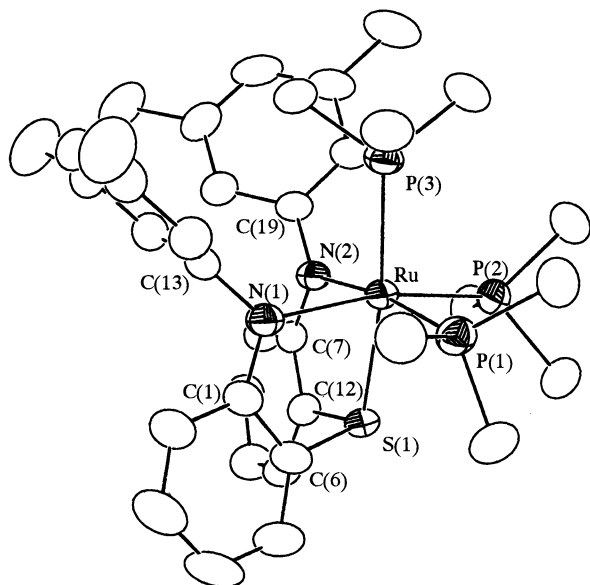


Figure 3. ORTEP diagram of **2** drawn at the 50% probability level. Hydrogen atoms are omitted for clarity.

Table 3. Selected Bond Lengths (Å) and Angles (deg) for [(PMe₃)₂LRu[Xy₂NSN]] (L = PMe₃ (2**), L = N₂H₄ (**5**))**

	2	5
Ru–N(1)	2.211(3)	2.158(3)
Ru–N(2)	2.204(3)	2.194(3)
Ru–S(1)	2.3262(9)	2.2748(10)
Ru–P(1)	2.2997(10)	2.2874(11)
Ru–P(2)	2.3450(10)	2.3145(11)
Ru–L	2.3901(10)	2.165(3)
N(3)–N(4)		1.479(5)
P(1)–Ru–P(2)	93.13(4)	96.88(4)
P(1)–Ru–L	91.00(3)	90.86(8)
P(2)–Ru–L	100.82(3)	95.80(9)
N(1)–Ru–N(2)	89.01(10)	86.43(11)
Ru–N(3)–N(4)		118.5(2)

resonance due to the PMe₃ ligands, and the ¹H NMR spectra exhibited a single PMe resonance as a weakly coupled virtual triplet. The infrared spectra of **3** showed an absorption band at 2257.2 cm⁻¹, which is characteristic of the end-on coordinated nitrile ligand. These features are consistent with substitution of the unique PMe₃ ligand in **2** by the nitrile ligand. Complex **3** may be an intermediate in the hydrogenation of benzonitrile with the **1a**/2PMe₃ catalyst system. Actually, the catalytic activity of **3** is almost comparable to that of **1a**/2PMe₃ (Table 2; entries 2 and 12).

Complex **2** also reacts with acetonitrile, a more weakly coordinating ligand than benzonitrile, to give an analogous nitrile complex [(PMe₃)₂(MeCN)Ru[Xy₂NSN]] (**4**) in good yield (eq 4). This has prompted us to examine the reaction of **2** with dinitrogen. When a solution of **2** in THF was treated with 30 atm of N₂ at room temperature for 48 h, a new absorption band was observed at 2164.9 cm⁻¹ with a weak intensity in the infrared spectrum of the solution just after the pressure of N₂ was decreased to 1 atm. This may indicate the formation of [(PMe₃)₂(N₂)Ru[Xy₂NSN]]. The band disappeared when the solution was bubbled with argon or kept for several hours under ambient N₂ pressure. The low conversion of **2** and the instability of the product prevented further characterization of the product.

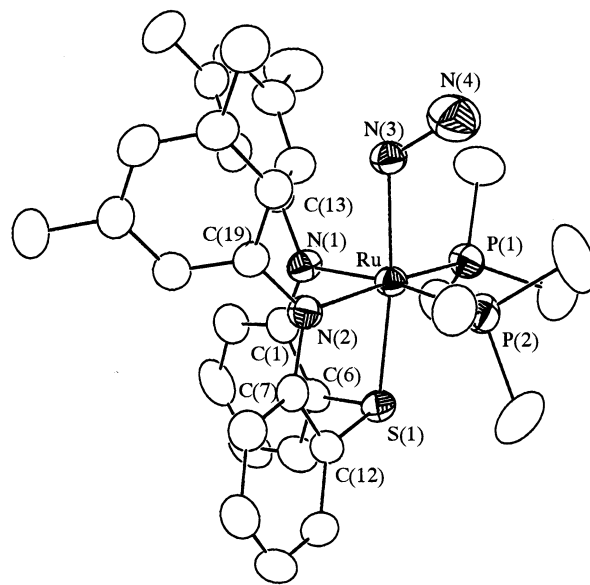
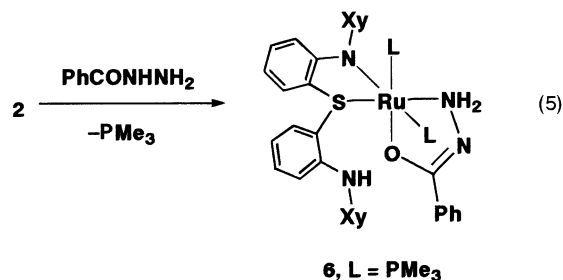


Figure 4. ORTEP diagram of **5** drawn at the 50% probability level. Hydrogen atoms are omitted for clarity.

We have also investigated the reaction of **2** with hydrazines. Similarly to the reaction of **2** with organonitriles, the reaction of **2** with hydrazine hydrate produced the bis(trimethylphosphine)–hydrazine complex [(PMe₃)₂(N₂H₄)Ru[Xy₂NSN]] (**5**) in 63% yield (eq 4). In the ¹H NMR spectrum of **5**, the NH protons gave rise to a multiplet at 3.94 ppm attributed to the Ru-bound NH₂ group and a broad triplet at 2.91 ppm (³J_{HH} = 4.4 Hz) assigned to the terminal NH₂ group. These features are consistent with the terminal end-on coordination of the hydrazine ligand. The structure of **5** was further confirmed by an X-ray analysis (Figure 4), and the selected structural parameters are listed in Table 3. When complex **2** was treated with benzoylhydrazine, the product was not a simple adduct but the κ²-benzoylhydrazido complex [(PMe₃)₂Ru(κ²-(O,N)-PhC(O)=NNH₂)(H[Xy₂NSN])] (**6**), which was isolated in 88% yield (eq 5). The ¹H NMR spectrum of **6** is consistent



with a formula that has no symmetry about ruthenium, and the ³¹P{¹H} NMR spectrum of **6** showed two doublet resonances at 17.7 and 12.4 ppm attributable to the two inequivalent PMe₃ ligands. The structure of **6** was determined by an X-ray analysis (Figure 5 and Table 4), which revealed the presence of a bidentate mono-amido/thioether H[Xy₂NSN]⁻ ligand with a dangling XyNHC₆H₄ arm. The η²-benzoylhydrazido ligand is bound to ruthenium with the oxygen and terminal nitrogen atoms forming a five-membered chelate ring. The N(3)–N(4) and C(35)–O(1) bonds are recognized as single bonds with bond lengths of 1.475(5) and 1.297(5)

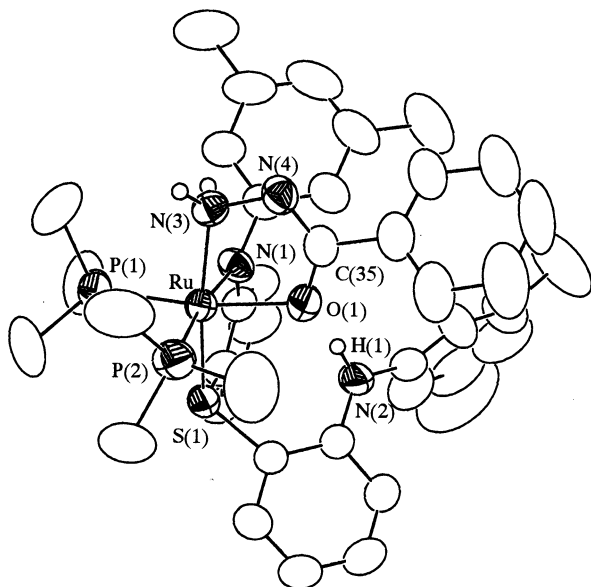


Figure 5. ORTEP diagram of **6** drawn at the 50% probability level. Hydrogen atoms except for the N–H hydrogen atoms are omitted for clarity.

Table 4. Selected Bond Lengths (Å) and Angles (deg) for **6**-(C₆H₁₄)_{0.5}·(C₆H₁₂)_{0.5}

Ru–N(1)	2.141(3)	Ru–O(1)	2.115(3)
Ru–S(1)	2.3137(11)	N(3)–N(4)	1.475(5)
Ru–P(1)	2.2629(12)	N(4)–C(35)	1.302(5)
Ru–P(2)	2.2848(12)	C(35)–O(1)	1.297(5)
Ru–N(3)	2.108(3)	O(1)···H(1)	2.121
N(1)–Ru–S(1)	82.51(9)	N(3)–N(4)–C(35)	110.5(3)
P(1)–Ru–P(2)	96.21(5)	Ru–O(1)–C(35)	112.2(2)
N(3)–Ru–O(1)	76.70(12)	O(1)–C(35)–N(4)	126.9(4)
Ru–N(3)–N(4)	113.6(2)	N(2)–H(1)···O(1)	144.4

Å, respectively, while the C(35)–N(4) bond length of 1.302(5) Å falls in the range of double-bond distances. The N–H hydrogen atom of the XyNHC₆H₄ moiety was found at the position close to the O(1) atom with an O(1)···H(1) distance of 2.121 Å and an N(2)–H(1)···O(1) angle of 144.4°, indicating the presence of an N–H···O hydrogen bond between these atoms.

Conclusion

We have synthesized new amidoruthenium complexes **1a** and **1b** by employing tridentate bis(diarylamido)/thioether ligands. Complexes **1a** and **1b** catalyze the hydrogenation of benzonitrile when combined with PCy₃. Although the catalytic activity of **1a**/2PCy₃ is comparable to that of the hydrido complex [RuH₂(η²-H₂)₂(PCy₃)₂], the finding that the product distribution is significantly affected by the kind of substituent on the amide ligands supports the catalysis of the amidoruthenium complex where the Ru–N bond is retained during the reaction. Complex **1a** reacts with excess trimethylphosphine to form [(PMe₃)₃Ru[Xy₂NSN]] (**2**). The PMe₃ ligand trans to the sulfur ligand is readily substituted by organonitriles and hydrazines. Our studies are in progress to elucidate the detailed mechanism of the hydrogenation of benzonitrile catalyzed by the amidoruthenium complexes.

Experimental Section

General Procedures. All manipulations except for the purification of the thioethers H₂[R₂NSN] (R = Xy, Xyf) were

performed under an inert atmosphere of nitrogen using standard Schlenk techniques. Toluene, hexanes, diethyl ether (Et₂O), and THF were dried over sodium benzophenone ketyl and distilled before use. Acetonitrile and dichloromethane were dried over P₂O₅ and distilled before use. Methanol was dried over magnesium methoxide and distilled before use. (H₂N-*o*-C₆H₄)₂S,⁹ [Pd(dba)₂] (dba = dibenzylideneacetone),¹⁸ [(η⁶-C₆H₆-RuCl₂)₂],¹⁹ and [RuH₂(η²-H₂)₂(PCy₃)₂]¹⁷ were prepared according to the literature, while other chemicals were commercially purchased and used as received. NMR spectra were recorded on a JEOL JNM-EX-400 spectrometer. IR spectra were recorded on a Shimadzu FTIR-8300 spectrometer. Elemental analyses were performed on a Perkin-Elmer 2400 series II CHN analyzer. High-resolution FABMS analyses were performed on a JEOL JMS600 instrument. Quantitative GLC analyses of organic compounds were performed on a Shimadzu GC-14B instrument equipped with a flame ionization detector using a 25 m × 0.25 mm CBP1 fused silica capillary column. GC–MS analyses were carried out on a Shimadzu GC-MS QP-5050 spectrometer.

Preparation of H₂[Xy₂NSN]. A 200 mL round-bottomed flask equipped with a magnetic stir bar and a nitrogen inlet was charged with (H₂N-*o*-C₆H₄)₂S (3.00 g, 13.9 mmol), [Pd(dba)₂] (400 mg, 0.696 mmol), *S*-BINAP (433 mg, 0.693 mmol), *t*-BuONa (2.94 g, 30.6 mmol), toluene (80 mL), and XyBr (5.14 g, 27.8 mmol). The reaction mixture was magnetically stirred at 80 °C for 18 h under a nitrogen atmosphere. After cooling to room temperature, the mixture was filtered and concentrated to a small volume on a rotary evaporator. The crude product was purified by silica gel column chromatography (hexanes–ethyl acetate). Evaporation of the band eluted with 5% ethyl acetate–hexanes gave H₂[Xy₂NSN] as a pale yellow oil. Yield: 4.50 g, 76%. HRFABMS calcd for C₂₈H₂₈N₂S: *m/e*, 424.19733; found 424.19693. ¹H NMR (400 MHz, CDCl₃): δ 7.31–7.28 (m, 4H, C₆H₄), 7.17, 6.82 (m, 2H each, C₆H₄), 6.68 (s, 4H, Me₂C₆H₃), 6.63 (s, 2H, Me₂C₆H₃), 6.30 (br s, 2H, NH), 2.25 (s, 12H, Me₂C₆H₃).

Preparation of H₂[Xyf₂NSN]. A 200 mL round-bottomed flask equipped with a magnetic stir bar and a nitrogen inlet was charged with (H₂N-*o*-C₆H₄)₂S (2.16 g, 9.99 mmol), [Pd(dba)₂] (288 mg, 0.50 mmol), *S*-BINAP (467 mg, 0.75 mmol), *t*-BuONa (2.10 g, 21.9 mmol), toluene (50 mL), and 3,5-bis-(trifluoromethyl)bromobenzene (5.86 g, 20.0 mmol). The reaction mixture was magnetically stirred at 80 °C for 3 days under a nitrogen atmosphere. After cooling to room temperature, the mixture was filtered and concentrated to a small volume on a rotary evaporator. The crude product was purified by column chromatography on alumina with diethyl ether as eluent to give H₂[Xyf₂NSN] as a dark red oil. Yield: 3.5 g, 55%. HRFABMS calcd for C₂₈H₁₆F₁₂N₂S: *m/e*, 640.08423; found 640.08421. ¹H NMR (CDCl₃): δ 7.27 (s, 2H, C₆H₃(CF₃)₂), 7.19–7.14 (m, 10H), 6.90 (dt, 2H, C₆H₄), 6.34 (s, 2H, NH). ¹³C{¹H} NMR (CDCl₃): δ 144.42, 140.84, 133.35, 129.59, 124.57, 124.35, 119.67, 116.50, 114.16, 132.83 (q, ²J_{CF} = 35 Hz, CF₃C), 123.83 (q, ¹J_{CF} = 273 Hz, CF₃).

Preparation of [(η⁶-C₆H₆)Ru[Xy₂NSN]] (1a**).** To a solution of H₂[Xy₂NSN] (2.72 g, 6.41 mmol) in THF (75 mL) was added a solution of *n*-BuLi (8.5 mL, 13.5 mmol; 1.59 M in *n*-hexane) at –78 °C, and the pale yellow solution was stirred at –78 °C for 30 min. Then, [(η⁶-C₆H₆)RuCl₂]₂ (1.61 g, 3.22 mmol) was added to the solution, and the mixture was slowly warmed to room temperature with stirring over 12 h and stirred at room temperature for 2 days to form a dark red solution. Solvents were evaporated, and the residue was extracted with dichloromethane (60 mL). Slow diffusion of MeOH to the concentrated extract afforded **1a** as dark red

(18) Ukai, T.; Kawazura, H.; Ishii, Y.; Bonnet, J. J.; Ibers, J. A. *J. Organomet. Chem.* **1974**, *65*, 253–266.

(19) Bennet, M. A.; Smith, A. K. *J. Chem. Soc., Dalton Trans.* **1974**, 233–241.

Table 5. Crystallographic Details for **1a**, **1b**·(CH₂Cl₂)_{0.5}, **2**, **5**, and **6**·(C₆H₁₄)_{0.5}·(C₆H₁₂)_{0.5}

	1a	1b ·(CH ₂ Cl ₂) _{0.5}	2	5	6 ·(C ₆ H ₁₄) _{0.5} ·(C ₆ H ₁₂) _{0.5}
empirical formula	C ₃₄ H ₃₂ N ₂ SRu	C _{34.5} H ₂₁ F ₁₂ ClSRu	C ₃₇ H ₅₃ N ₂ P ₃ SRu	C ₃₄ H ₄₈ N ₄ P ₂ SRu	C ₄₇ H ₆₅ N ₄ OP ₂ SRu
fw	601.75	860.11	751.85	707.83	897.10
cryst size (mm)	0.55 × 0.15 × 0.03	0.50 × 0.30 × 0.10	0.55 × 0.15 × 0.03	0.40 × 0.10 × 0.10	0.80 × 0.25 × 0.20
cryst syst	monoclinic	monoclinic	monoclinic	monoclinic	monoclinic
<i>a</i> (Å)	17.355(7)	34.251(2)	12.440(3)	17.236(6)	14.466(4)
<i>b</i> (Å)	8.359(3)	8.7147(4)	16.292(4)	11.625(4)	21.312(6)
<i>c</i> (Å)	20.938(8)	22.8057(15)	19.821(5)	18.245(6)	16.090(5)
β (deg)	110.701(4)	100.658(3)	112.051(3)	108.639(4)	103.387(4)
<i>V</i> (Å ³)	2841.2(19)	6689.8(7)	3723.3(15)	3464(2)	4826(3)
space group	<i>P</i> 2 ₁ / <i>n</i>	<i>C</i> 2/ <i>c</i>	<i>P</i> 2 ₁ / <i>c</i>	<i>P</i> 2 ₁ / <i>a</i>	<i>P</i> 2 ₁ / <i>n</i>
<i>Z</i>	4	8	4	4	4
<i>D</i> _{calc} (g/cm ³)	1.407	1.708	1.341	1.357	1.235
abs coeff (mm ⁻¹)	0.651	0.708	0.634	0.634	0.471
<i>F</i> ₀₀₀	1240	3416	1576	1480	1892
no. of reflns collected	20 436	23 909	27 233	25 280	35 542
no. of ind reflns	6481	7248	8392	7861	11 018
goodness of fit on <i>F</i> ²	1.171	1.105	1.047	1.062	1.049
R1 [<i>I</i> > 2σ(<i>I</i>)]	0.0615	0.0473	0.0464	0.0502	0.0621
wR2 (all data)	0.1078	0.1118	0.1141	0.1152	0.1606
largest diff peak and hole (e Å ⁻³)	0.36 and -0.28	0.87 and -0.52	0.99 and -0.41	0.60 and -0.37	1.04 and -0.36

crystals. Yield: 2.40 g, 62%. Anal. Calcd for C₃₄H₃₂N₂SRu: C, 67.86; H, 5.36; N, 4.66. Found: C, 67.57; H, 5.35; N, 4.63. ¹H NMR (400 MHz, C₆D₆): δ 7.65 (d, 2H, C₆H₄), 6.79–6.70 (m, 4H, C₆H₄), 6.34 (t, 2H, C₆H₄), 6.78 (s, 4H, Me₂C₆H₃), 6.72 (s, 2H, Me₂C₆H₃), 4.41 (s, 6H, C₆H₆), 2.23 (s, 12H, Me₂C₆H₃).

Preparation of [(η^6 -C₆H₆)Ru(Xy₂NSN)]·0.5CH₂Cl₂ (1b**·(CH₂Cl₂)_{0.5}).** To a solution of H₂[Xy₂NSN] (0.108 g, 0.169 mmol) in THF (8 mL) was added a solution of *n*-BuLi (234 μ L, 0.374 mmol; 1.6 M in *n*-hexane) at -78 °C, and the orange solution was stirred at -78 °C for 30 min. To this was added [(η^6 -C₆H₆)RuCl₂]₂ (42 mg, 0.0840 mmol), and the mixture was slowly warmed to room temperature with stirring over 12 h to form a dark red solution. Solvents were evaporated, and the residue was extracted with dichloromethane (ca. 10 mL). The dichloromethane extract was loaded on a column of alumina and then eluted with diethyl ether to give a red band, which was collected and evaporated to dryness. Recrystallization of the red solid from dichloromethane–hexanes afforded **1b**·(CH₂Cl₂)_{0.5} as dark red crystals. Yield: 55 mg, 38%. Anal. Calcd for C₃₄H₂₀N₂F₁₂SRu·0.5CH₂Cl₂: C, 48.18; H, 2.46; N, 3.26. Found: C, 48.01; H, 2.38; N, 3.17. ¹H NMR (400 MHz, C₆D₆): δ 7.57 (s, 2H, C₆H₃(CF₃)₂), 7.46 (d, 2H, C₆H₄), 7.20 (br s, 4H, C₆H₃(CF₃)₂), 6.63 (t, 2H, C₆H₄), 6.45 (d, 2H, C₆H₄), 6.34 (t, 2H, C₆H₄), 4.11 (s, 6H, C₆H₆).

Preparation of [(PMe₃)₃Ru(Xy₂NSN)]·(THF)₂ (2**·(THF)₂).** To a solution of **1a** (600 mg, 1.0 mmol) in DMF (23 mL) was added a solution of PMe₃ in toluene (1.0 M, 10 mL), and the mixture was heated at 80 °C for 2 days to form a yellow solution. Volatiles were removed in vacuo, and the residual solid was recrystallized from hot THF (10 mL) to give **2**·(THF)₂ as yellow crystals. Yield: 650 mg, 73%. Single crystals of **2** suitable for X-ray diffraction study were obtained by recrystallization from toluene–hexanes. Anal. Calcd for C₃₇H₅₃N₂P₃SRu·2C₄H₈O: C, 60.32; H, 7.76; N, 3.13. Found: C, 60.17; H, 7.73; N, 3.19. ¹H NMR (C₆D₆): δ 7.82 (dd, 2H, C₆H₄), 6.96 (dt, 2H, C₆H₄), 6.95 (br s, 4H, Me₂C₆H₃), 6.86 (dd, 2H, C₆H₄), 6.66 (s, 2H, Me₂C₆H₃), 6.39 (dt, 2H, C₆H₄), 2.23 (s, 12H, Me₂C₆H₃), 1.11 (vt, 18H, PMe₃), 0.53 (d, 9H, PMe₃). ³¹P{¹H} NMR (C₆D₆): δ 2.2 (d, *J* = 33.1 Hz, 2P), -12.9 (t, *J* = 29.4 Hz, 1P).

Preparation of [(PMe₃)₂(PhCN)Ru(Xy₂NSN)] (3**).** To a solution of **2**·(THF)₂ (90 mg, 0.10 mmol) in toluene (5 mL) was added benzonitrile (206 mg, 2.0 mmol), and the mixture was stirred at room temperature for 18 h. Volatiles were removed in vacuo, and the residue was recrystallized from boiling acetone to give **3** as an orange crystalline solid. Yield: 38 mg, 49%. Anal. Calcd for C₄₁H₄₉N₃P₂SRu: C, 63.22; H, 6.34; N, 5.39. Found: C, 62.57; H, 6.39; N, 5.71. ¹H NMR (C₆D₆): δ 7.39 (m, 1H, Ph), 7.37 (m, 2H, Ph), 7.34 (m, 2H, C₆H₄), 7.01

(m, 2H, Ph), 6.64 (m, 2H, C₆H₄), 6.49 (d, 2H, C₆H₄), 6.38 (br s, 4H, Me₂C₆H₃), 6.35 (s, 2H, Me₂C₆H₃), 6.00 (t, 2H, C₆H₄), 1.91 (s, 12H, Me₂C₆H₃), 1.28 (vt, 18H, PMe₃). ³¹P{¹H} NMR (CD₂Cl₂): δ 9.2 (s). IR (KBr): 2257.2 (ν (C=N)) cm⁻¹.

Preparation of [(PMe₃)₂(MeCN)Ru(Xy₂NSN)] (4**).** A suspension of **2**·(THF)₂ (448 mg, 0.50 mmol) in MeCN (35 mL) was stirred at 60 °C for 14 h to form a yellow suspension. The mixture was heated at reflux to give a yellow solution, from which yellow crystals of **4** were obtained on cooling to -30 °C. Yield: 259 mg, 72%. Anal. Calcd for C₃₆H₄₇N₃P₂SRu: C, 60.32; H, 6.61; N, 5.86. Found: C, 60.21; H, 6.69; N, 6.11. ¹H NMR (C₆D₆): δ 7.75 (dd, 2H, C₆H₄), 7.13 (dd, 2H, C₆H₄), 6.93 (dt, 2H, C₆H₄), 6.61 (br s, 4H, Me₂C₆H₃), 6.56 (s, 2H, Me₂C₆H₃), 6.39 (dt, 2H, C₆H₄), 2.14 (s, 12H, Me₂C₆H₃), 1.06 (vt, 18H, PMe₃), 0.96 (s, 3H, MeCN). ³¹P{¹H} NMR (C₆D₆): δ 9.4 (s). IR (KBr): 2266.2 (ν (C=N)) cm⁻¹.

Preparation of [(PMe₃)₂(N₂H₄)Ru(Xy₂NSN)] (5**).** To a solution of **2**·(THF)₂ (100 mg, 0.11 mmol) in THF (5 mL) was added N₂H₄·H₂O (56 mg, 1.1 mmol), and the mixture was stirred at 60 °C for 18 h. Volatiles were removed in vacuo, and the residue was recrystallized from dichloromethane–hexanes to give **5** as a yellow crystalline solid. Yield: 49 mg, 63%. Anal. Calcd for C₃₄H₄₈N₄P₂SRu: C, 57.69; H, 6.83; N, 7.92. Found: C, 57.74; H, 6.76; N, 7.80. ¹H NMR (CD₂Cl₂): δ 7.37 (dd, 2H, C₆H₄), 6.65 (dt, 2H, C₆H₄), 6.51 (s, 2H, Me₂C₆H₃), 6.50 (dd, 2H, C₆H₄), 6.39 (s, 4H, Me₂C₆H₃), 6.06 (dt, 2H, C₆H₄), 3.94 (m, 2H, RuNH₂NH₂), 2.91 (br t, ³J_{HH} = 4.4 Hz, 2H, RuNH₂NH₂), 2.18 (br s, 12H, Me₂C₆H₃), 1.29 (vt, 18H, PMe₃). ³¹P{¹H} NMR (CD₂Cl₂): δ 9.0 (s).

Preparation of [(PMe₃)₂Ru(κ^2 -(*O,N*)-PhC(O)=NNH₂)-(H[Xy₂NSN])] (6**).** To a solution of **2**·(THF)₂ (65 mg, 0.073 mmol) in toluene (5 mL) was added benzoylhydrazine (14 mg, 0.10 mmol), and the mixture was stirred at 60 °C for 2 days. Volatiles were removed in vacuo, and the residue was recrystallized from THF–hexanes to give **6** as yellow crystals. Yield: 52 mg, 88%. Anal. Calcd for C₄₁H₅₂N₄OP₂SRu: C, 60.65; H, 6.46; N, 6.90. Found: C, 60.94; H, 6.61; N, 7.24. ¹H NMR (CD₂Cl₂): δ 8.01 (br s, 1H, XyNH), 7.77 (m, 1H, C₆H₄), 7.67 (d, 2H, Ph), 7.32 (t, 1H, Ph), 7.25 (dt, 1H, Ph), 7.24 (m, 2H, C₆H₄), 6.92 (dd, 1H, C₆H₄), 6.81 (dt, 1H, C₆H₄), 6.68 (s, 1H, Me₂C₆H₃), 6.49 (dt, 1H, C₆H₄), 6.39 (br s, 2H, Me₂C₆H₃), 6.30 (s, 1H, Me₂C₆H₃), 6.17 (br s, 2H, Me₂C₆H₃), 6.01 (dd, 1H, C₆H₄), 5.95 (dt, 1H, C₆H₄), 5.32 (m, 1H, NNH₂), 4.95 (dd, 1H, NNH₂), 2.31, 1.90 (br s, 3H each, Me₂C₆H₃), 1.88 (s, 6H, Me₂C₆H₃), 1.26, 1.17 (d, 9H each, PMe₃). ³¹P{¹H} (CD₂Cl₂): δ 17.7 (d, *J* = 33.1 Hz), 12.4 (d, *J* = 33.1 Hz).

Hydrogenation of Benzonitrile. A typical procedure for the hydrogenation of benzonitrile is as follows. A THF solution

(5 mL) containing complex **1a** (30 mg, 0.050 mmol), PCy₃ (28 mg, 0.10 mmol), and benzonitrile (516 mg, 5.00 mmol) was prepared in a Schlenk tube and then transferred to a 50 mL stainless steel autoclave by syringe. The reactor was pressurized with H₂ (30 atm) at room temperature, and the reaction mixture was heated at 80 °C with stirring for 18 h. After the mixture was cooled to room temperature, hydrogen gas was released and the products were analyzed by gas chromatography.

X-ray Crystal Structure Determination of 1b·(CH₂Cl₂)_{0.5}, 2, 5, and 6·(n-C₆H₁₄)_{0.5}·(cyclo-C₆H₁₂)_{0.5}. Single crystals suitable for X-ray diffraction study were sealed in a glass capillary and used for data collection. All measurements were performed on a Rigaku MercuryCCD system. A total of 720 oscillation images were collected at 20 °C with the exposure rate of 15 s for each still. The data reductions were performed using Rigaku CrystalClear program. Empirical absorption correction and Lorentz–polarization corrections were applied.

The structures were solved by direct method (SIR 92)²⁰ and refined by full-matrix least-squares method on F^2

(20) Altomare, A.; Cascarano, G.; Giacovazzo, C.; Guagliardi, A. *J. Appl. Crystallogr.* **1993**, *26*, 343–350.

(21) Sheldrick, G. M. *SHELXL-97, Program for Crystal Structure Refinement*; University of Göttingen: Göttingen, Germany, 1997.

(SHELXL97).²¹ All non-hydrogen atoms were refined with anisotropic thermal parameters. All C–H hydrogen atoms were placed at the calculated positions and treated as riding models. The N–H hydrogen atoms in **6**·(n-C₆H₁₄)_{0.5}·(cyclo-C₆H₁₂)_{0.5} were found in the difference Fourier map and were refined isotropically, while those in **5** were not found and were not included in the calculation. For **1b**·(CH₂Cl₂)_{0.5}, the two CF₃ groups in one of the two Xyf substituents were disordered and were modeled with six fluorine atoms (50% occupancy) for each CF₃ group. Details of the crystallographic parameters are summarized in Table 5.

Acknowledgment. This work was supported by the JSPS FY2000 and FS2001 “Research for the Future Program”. We thank Dr. Hidetake Seino at The University of Tokyo for assistance with FABMS analyses.

Supporting Information Available: Tables giving X-ray crystallographic data for **1a**, **1b**·(CH₂Cl₂)_{0.5}, **2**, **5**, and **6**·(n-C₆H₁₄)_{0.5}·(cyclo-C₆H₁₂)_{0.5}. This material is available free of charge via the Internet at <http://pubs.acs.org>.

OM0203400